International Journal of Heat and Mass Transfer 77 (2014) 301–310

Contents lists available at ScienceDirect

International Journal of Heat and Mass Transfer

journal homepage: www.elsevier.com/locate/ijhmt

Utilization of orthotropic graphite plates in plate heat exchangers, analytical modeling

Farshid Bagheri *, M. Fakoor-Pakdaman, Majid Bahrami

Laboratory for Alternative Energy Conversion (LAEC), School of Mechatronic Systems Engineering, Simon Fraser University, Surrey, BC V3T 0A3, Canada

ARTICLE INFO

Article history:
Received 24 February 2014
Received in revised form 2 May 2014
Accepted 9 May 2014

Keywords:
Orthotropic media
Graphite sheet
Plate heat exchanger
Effectiveness
Critical conductivity

ABSTRACT

Recently developed graphite plates with large in-plane thermal conductivity are considered as promising alternative to conventional metallic plate heat exchangers (PHE). A new analytical model is developed to study the impact, and the potentials, of the emerging orthotropic graphite-based plates in PHE under various convective regimes. Closed-form relationships are obtained for temperature and heat flux distributions, and applied to perform a comprehensive parametric study on the orthotropic conductivity effects. Our results show that increasing the in-plane thermal conductivity leads to significant changes in heat flow pattern and reduction in temperature variation along the plate. In spite of the remarkable effects of in-plane thermal conductivity on the heat flow pattern, through-plane thermal conductivity plays the key role in controlling the total heat transfer between the hot and cold fluid streams through the plate. Moreover, a new critical through-plane conductivity is proposed to calculate the maximum value of thermal conductivity that provides the highest heat transfer rate through orthotropic slabs. The critical value also includes convective heat transfer resistance of the fluid side and the plate thickness effects. To verify the present model, an independent numerical study is conducted using COMSOL Multiphysics. The analytical results are compared with the obtained numerical data as well as an existing data set in the literature and show a great agreement with less than 5% relative difference.

1. Introduction

Plate heat exchangers (PHE) are one of the main apparatus in which the conductive flat plates are directly utilized as the medium for transferring heat between any combination of gas, liquid, and two-phase streams. PHE are widely used in an array of engineering applications such as: air conditioning and refrigeration (A/C–R), power plants, solar collectors, dairy and food processing plants, to achieve high heat transfer effectiveness [1–5]. They exhibit excellent heat transfer characteristics, which allow for compact design, easy assembly/dismounting for maintenance, and modifying the heat transfer area by adding or removing the plates. PHE feature compactness (low volume/surface ratio), high overall heat transfer coefficients, and low production and operational costs [6–8].

Conventional heat exchangers are mainly constructed from monolithic metals and metal alloys, e.g. aluminum and copper. However, the metallic heat exchangers cannot operate at high temperatures for extended periods of time; they foul when operated in corrosive environments; and thermal shock shortens their life. These conditions can occur in many thermal management systems [9]. Emergence of new manufacturing processes such as roll-embossing makes patterning of graphite plates competitive with the existing metallic sheets. As such, graphite-based PHE can potentially be considered as an alternative due to their superior performance and thermal characteristics.

Graphite is inert throughout its entire structure, stable over a wide range of temperature, sublimating at about 3900 K and melting at about 4800 K under atmospheric conditions, and resistant to most common corrosive reagents [10,11]. Moreover, graphite has a low density compared to metals and alloys (graphite: 2.1 g/cm^3, aluminum: 2.7 g/cm^3) which makes it an ideal candidate for compact and lightweight applications [10–13]. In addition, using graphite sheets – featuring large in-plane thermal conductivity values (800–1000 W/m/K) and through-plane values on the order of 10 W/m/K [14–18] – to manufacture PHE, is an exceptional opportunity to improve the heat exchanger effectiveness. Fig. 1 shows a SEM of a graphite sheet.

A compressed graphite sheet consists of graphene layers with high thermal conductivity. Thermal contact resistance between the graphene layers results in a rather low through-plane thermal conductivity of the graphite sheets. Accordingly, the objective of

* Corresponding author. Tel.: +1 778 782 8538.
E-mail addresses: fbagheri@sfu.ca (F. Bagheri), mbahrami@sfu.ca (M. Bahrami).

http://dx.doi.org/10.1016/j.ijheatmasstransfer.2014.05.013
0017-9310/

Nomenclature

Symbols

T	temperature K
k	thermal conductivity W/m/K
h	convective heat transfer coefficient W/m^2/K
a	plate thickness m
b	plate height m
ΔT	flow temperature drop K
q''	heat flux W/m^2
Q	total heat transfer per unit depth of plate W/m
R	thermal resistance m K/W
C_i	series solution constant
C_i'	series solution constant
D_i	series solution constant
n	series solution variable
γ	solution constant
λ	solution constant
f	surface heat flux function
g	surface heat flux function

Subscripts

in	inlet
out	outlet
c	cold flow
h	hot flow
x	*x* direction
y	*y* direction
m	mean (fluid bulk)

Superscript

*	dimensionless parameters script

this study is to investigate the suitability of graphite-based plates for PHE applications.

Progress in the thermal modeling and analysis of PHE has been significant in the last decades due to their simple geometry and well established flow conditions [7]. There are several publications on the lumped thermodynamic modeling of PHE [8,19–21] and investigations through the convective heat transfer for different arrangements of this kind of heat exchangers [7,8,22–26]. However, there are only limited studies available on the conductive heat transfer inside the plates of PHE. For investigating the conductive/convective heat transfer characteristics of PHE, modeling the flat plate heat transfer has been the most appropriate analysis methodology [1–3]. Mehrabian [27] and Mehrabian et al. [28] developed analytical solutions for temperature distribution within an isotropic PHE and studied uniform heat flux for constant overall heat transfer coefficient. Grine et al. [29] studied a transient one-dimensional heat transfer through a thin isotropic plate analytically and experimentally. The plate was exposed to a convective heat transfer on one face and to a position-independent heat flux on the other side. Beck et al. [30] developed an analytical model for two-dimensional heat transfer through a rectangular plate with constant temperature boundary conditions.

A number of studies were focused on the thermo-mechanical behavior of orthotropic materials. As a result of emerging applications of orthotropic materials in engineering systems, analytical solutions for multidimensional heat conduction in layered media have attracted considerable attention recently. Heltzel et al. [11] numerically studied the thermal behavior of finned plate heat exchangers made from orthotropic graphite fins. They reported that the graphite-based heat exchanger outperforms a similar heat exchanger made from aluminum, rejecting more than 20% more heat from the hot flow stream (water) to the cold flow streams (air) at Reynolds numbers of 3000–4000. Nemirovskii et al. [31] carried out an asymptotic solution for steady heat conduction through multilayered orthotropic plates. The asymptotes were defined as different boundary conditions on plate walls: constant heat flux, constant temperature, and convective heat transfer with constant temperature fluid streams. Hsieh et al. [32] analytically solved two-dimensional heat conduction in an orthotropic thin-layer containing heat sources which was embedded between two half-planes with constant temperatures.

The abovementioned literature review indicates that the heat conduction in orthotropic plates has not been studied in-depth, and the pertinent literature lacks the following:

- Analytical thermal model for orthotropic plates that covers location-dependent heat flux boundary condition.
- Critical through-plane conductivity that provides the maximum heat transfer rate through the slab for different convective heat transfer applications, e.g. natural convection, forced convection, and two-phase flow.

The present study aims to develop a new analytical thermal model for orthotropic plates exposed to "location-dependent heat flux". The main goal is to simulate various PHE applications and ultimately investigate, and establish, suitable applications for graphite-based plates. To develop the thermal model, a separation of variables approach is applied. The temperature and heat flux distributions are obtained in the form of Fourier's series. The model is then employed to perform a parametric study to investigate the effects of orthotropic conductivity on heat transfer characteristics of PHE. A new criterion for critical through-plane conductivity of PHE is defined and correlated to the fluid-side's convective resistance. To verify the developed model, an independent numerical

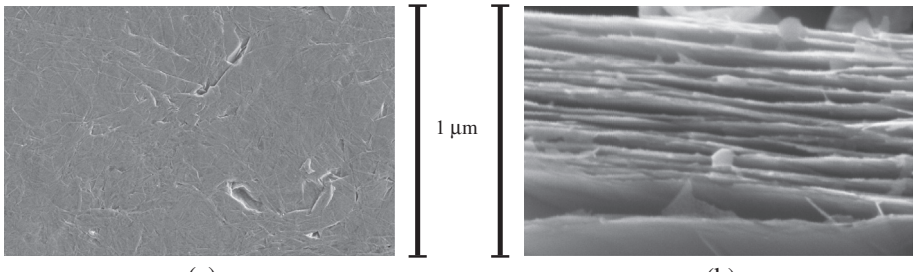

Fig. 1. SEM of graphite sheet (a) top view, (b) cross section view.

study using COMSOL Multiphysics is performed. Then the obtained numerical results as well as existing data from Beck et al. [30] are utilized to verify the analytical model.

2. Analytical model development

A schematic of an orthotropic slab, as a representative of a typical PHE, is presented in Fig. 2. The symmetry lines in Fig. 2 demarcate the region between neighboring plates; as such the analysis can be performed for one plate without losing generality. The plate material is orthotropic, e.g. graphite sheet, with different thermal conductivities in x and y directions (k_x, k_y). The following assumptions are made for the model development:

- Two-dimensional heat transfer, negligible variations in the z-direction.
- The heat flux changes in y-direction due to temperature variations in fluid streams.
- Different mass flow rates for the hot and cold streams to set various convective heat transfer coefficient, following [33].
- Known temperature distribution inside the fluid domain: $T_c(y)$, $T_h(y)$, this is to decouple the hot/cold fluid streams convective heat transfers from the conduction inside the plate.
- Constant fluid properties.

The energy equation for the plate will then become [2,3]:

$$k_x\frac{\partial^2 T(x,y)}{\partial x^2}+k_y\frac{\partial^2 T(x,y)}{\partial y^2}=0 \tag{1}$$

Eq. (1) is subjected to the following boundary conditions:

$$\begin{cases} @\,y=0,b: & \frac{\partial T(x,y)}{\partial y}=0 \\ @\,x=0: & -k_x\frac{\partial T(x,y)}{\partial x}=f(y)=h_c(T_c(y)-T(x,y)) \\ @\,x=a: & -k_x\frac{\partial T(x,y)}{\partial x}=g(y)=h_h(T(x,y)-T_h(y)) \end{cases} \tag{2}$$

Using the two homogeneous boundary conditions at $y=0$, and $y=b$, the solution of the partial differential Eq. (1) is obtained by applying a method of separation of variables [2]. The general solution is as follows:

$$\begin{aligned} T(x,y)=&(C_1x+C_2)(D_1y+D_2)\\ &+\left(C_3\sinh\left(\frac{\lambda}{\sqrt{k_x}}x\right)+C_4\cosh\left(\frac{\lambda}{\sqrt{k_x}}x\right)\right)\\ &\times\left(D_3\sin\left(\frac{\lambda}{\sqrt{k_y}}y\right)+D_4\cos\left(\frac{\lambda}{\sqrt{k_y}}y\right)\right)\\ &+\left(C_5\sin\left(\frac{\gamma}{\sqrt{k_x}}x\right)+C_6\cos\left(\frac{\gamma}{\sqrt{k_x}}x\right)\right)\\ &\times\left(D_5\sinh\left(\frac{\gamma}{\sqrt{k_y}}y\right)+D_6\cosh\left(\frac{\gamma}{\sqrt{k_y}}y\right)\right) \end{aligned} \tag{3}$$

By applying the $y=0$, and $y=b$ boundary conditions on Eq. (3), D_1, D_3, D_5, D_6 constants drop. Substituting these constants into Eq. (3)leads to a general solution for the temperature distribution with the eigenvalues shown in Eqs. (4) and (5).

$$\begin{aligned} T(x,y)=&(C_1'x+C_2')\\ &+\sum_{n=1}^{\infty}\left[\left(C_n\cosh\left(\frac{n\pi}{b}\sqrt{\frac{k_y}{k_x}}x\right)+D_n\sinh\left(\frac{n\pi}{b}\sqrt{\frac{k_y}{k_x}}x\right)\right)\cos\left(\frac{n\pi}{b}y\right)\right] \end{aligned} \tag{4}$$

$$\lambda=\frac{n\pi}{b}\sqrt{k_y} \tag{5}$$

Before applying the other boundary conditions, the fluid side temperature distributions should be known. The convective boundary conditions at $x=0$, a presented in Eq. (2) are called boundary conditions of the third kind [1]. In conjugate heat transfer problems through which both the solid and fluid domains are solved simultaneously, the fluid side's heat transfer equation is used as an additional equation. Then, both the fluid and solid sides of any common fluid–solid boundary are found from the solution. Although some simpler versions of plate heat exchanger models have been analytically solved and presented in the open literature [30,33,34], solving a more realistic model, like the current study's model, using the available exact analytical methods is too difficult or even impossible. Since the aim of the present study is focusing on the effects of orthotropicity of the plate on heat transfer domain, the fluid sides' heat transfer characteristics are assumed as known. Therefore, $T_{h,in}$, $T_{h,out}$, $T_{c,in}$, $T_{c,out}$ as well as the convective heat transfer coefficients for both streams are known. Based on the known inlet and outlet fluid temperature changes (ΔT_c and ΔT_h), linear profiles for average fluid temperature along the channels are assumed. Accordingly, the known $f(y)$ and $g(y)$ functions are defined as follows:

$$\begin{cases} f(y)=h_c\left(\frac{\Delta T_c}{b}y+T_{c,out}-T(0,y)\right) \\ g(y)=h_h\left(T(a,y)-\frac{\Delta T_h}{b}y-T_{h,in}\right) \end{cases} \tag{6}$$

By applying the boundary conditions at $x=0$, and $x=a$ followed by using the orthogonality of cosine functions, and after some algebraic steps, the unknown coefficients; C_1', C_2', C_n, and D_n, are determined as follows:

$$\begin{cases} C_1'=\frac{\bar{h}_h}{k_x+a\bar{h}_h+\frac{b\bar{h}_h}{\bar{h}_c}k_x}\left(\frac{\Delta T_h-\Delta T_c}{2}+T_{h,in}-T_{c,out}\right) \\ C_2'=\frac{k_x\bar{h}_h}{\bar{h}_c\left(k_x+a\bar{h}_h+\frac{b\bar{h}_h}{\bar{h}_c}k_x\right)}\left(\frac{\Delta T_h-\Delta T_c}{2}+T_{h,in}-T_{c,out}\right)+\frac{\Delta T_c}{2}+T_{c,out} \\ C_n=\left(\frac{\frac{2\bar{h}_c\Delta T_c}{n^2\pi^2}\cosh(C^*)+\frac{2b\bar{h}_h\bar{h}_c\Delta T_c}{n^3\pi^3\sqrt{k_xk_y}}\sinh(C^*)+\frac{2\bar{h}_h\Delta T_h}{n^2\pi^2}}{\left(\frac{n\pi\sqrt{k_xk_y}}{b}+\frac{b\bar{h}_h\bar{h}_c}{n\pi\sqrt{k_xk_y}}\right)\sinh(C^*)+(\bar{h}_h+\bar{h}_c)\cosh(C^*)}\right)(\cos(n\pi)-1) \\ D_n=\left(\left(\frac{\frac{2\bar{h}_c\Delta T_c}{n^2\pi^2}\cosh(C^*)+\frac{2b\bar{h}_h\bar{h}_c\Delta T_c}{n^3\pi^3\sqrt{k_xk_y}}\sinh(C^*)+\frac{2\bar{h}_h\Delta T_h}{n^2\pi^2}}{\left(\frac{n\pi\sqrt{k_xk_y}}{b}+\frac{b\bar{h}_h\bar{h}_c}{n\pi\sqrt{k_xk_y}}\right)\sinh(C^*)+(\bar{h}_h+\bar{h}_c)\cosh(C^*)}\right)-\frac{2\Delta T_c}{n^2\pi^2}\right)\frac{b\bar{h}_c}{n\pi\sqrt{k_xk_y}}(\cos(n\pi)-1) \end{cases} \tag{7}$$

where, C^* is defined in Eq. (8).

$$C^*=\frac{n\pi a}{b}\sqrt{\frac{k_y}{k_x}} \tag{8}$$

After finding temperature distribution in orthotropic plates, heat flux can be calculated from Eq. (9). In addition, conductive thermal resistance of the plate can be calculated using Eq. (10).

$$\begin{cases} q_x''=-k_x\frac{\partial T(x,y)}{\partial x} \\ q_y''=-k_y\frac{\partial T(x,y)}{\partial y} \end{cases} \tag{9}$$

$$R_{conduction,plate}=\frac{\Delta\bar{T}}{Q}=\frac{\bar{T}_{x=0}-\bar{T}_{x=a}}{\int_0^b\left(-k_x\frac{\partial T}{\partial x}\big|_{x=0}\right)dy} \tag{10}$$

Since the top and bottom surfaces of the plate (i.e. $y=0$, and $y=b$) are insulated, the total heat flow at any cross section, $x=constant$, is the same to satisfy the energy equation. Accordingly, the total heat flow in Eq. (10) can be calculated at any arbitrary section, e.g., $x=0$. Furthermore, to find the total thermal resistance of the plate from Eq. (10), the average surface temperatures at $x=0$, and $x=a$, should be calculated. The results of these calculations are presented in Eq. (11). Accordingly, the conductive thermal

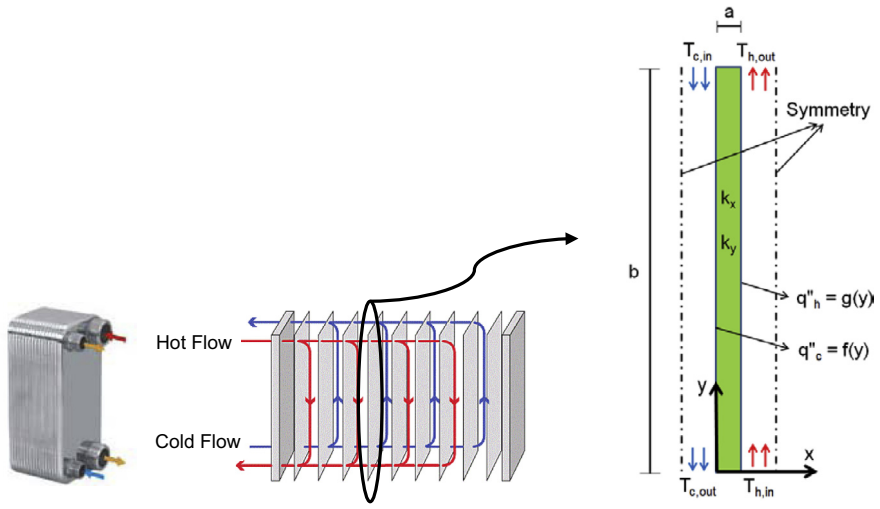

Fig. 2. Schematic representation of the PHE model.

resistance of the considered orthotropic plate is shown in Eq. (12). From Eq. (12), it can be found that although k_y appears in the temperature distribution correlation, k_x plays the key role for total thermal conductivity of the plate between the two streams.

$$\begin{cases} \bar{T}_{x=0} = \frac{1}{b}\int_0^b T(0,y)dy = C_2' \\ \bar{T}_{x=a} = \frac{1}{b}\int_0^b T(a,y)dy = C_1'a + C_2' \\ Q = \int_0^b \left(-k_x \frac{\partial T}{\partial x}\big|_{x=0}\right)dy = -C_1' b k_x \end{cases} \tag{11}$$

$$R_{conduction,plate} = \frac{a}{bk_x} \tag{12}$$

3. Numerical model development

In addition to the developed analytical solution, an independent numerical simulation of the orthotropic plate exposed to the same variable heat flux boundary conditions, shown in Fig. 2, is conducted. COMSOL Multiphysics is used for the numerical simulation of the model. The conduction heat transfer module in COMSOL is employed to determine the temperature distribution and heat transfer domain. All the assumptions described in Section 2 are used for the numerical simulations. To conduct the numerical study, typical baseline geometrical properties for a plate used in PHE and its thermo-physical/operational properties of the fluid sides are considered based on a water to water PHE [4–6]. Using the available common working conditions information, the baseline parameters are presented in Table 1 [26,33]. It should be mentioned that both the hot and cold fluids are assumed water and the plate is built from graphite sheets. The mesh independency is tested by investigating various elements 100×20, 200×50, 500×80; the results show relative discrepancy less than 10^{-3}.

4. Analytical model verification

To verify the obtained analytical model, the numerical results from COMSOL modeling as well as the results from Beck et al. [30] are used. A part of the verification can be found in Section 5 where Figs. 6 and 7 show a good agreement between the analytical and numerical results with less than 4% discrepancy for the temperature and heat flux distributions. Moreover, in Fig. 3 a comparison between justified versions of both the analytical and numerical models of the present study with results from Beck et al. [30] for the same boundary condition, constant surface temperature and $k_x = k_y = 11$ W/m/K, is presented. Since no similar analytical and experimental models were found in the literature for a plane orthotropic plate exposed to realistic location-dependent heat flux, the closest available model from Beck et al. is considered for verification. To do so, the x and y direction thermal conductivity values in the current model are set equal (i.e. isotropic plate) and the boundary conditions are changed from location-dependent heat flux to constant wall temperatures, see Ref. [30]. The presented results in Fig. 3 show a good agreement of the adapted version of the present analytical model with the obtained numerical data and Beck et al. results with a maximum of 5% difference.

It should be mentioned that since both the analytical and numerical models are developed based on the same energy equation with the same boundary conditions, a good agreement was expected to be achieved. For the numerical simulations, the COMSOL's module of "heat transfer in solids" is employed through which a location-dependent heat flux is imposed on each of the plate's fluid–solid common walls. To do so, the stream bulk temperatures from Eq. (6) are defined as the external temperature source for the walls. The small discrepancy between the analytical and numerical results is as a result of finite element approximation in numerical solution in COMSOL. Indeed, while the continuous solid domain is solved by the analytical model, a discretized domain is solved by the numerical solver.

5. Parametric study

A parametric study is performed to investigate the effects of salient parameters of orthotropic plates on thermal performance

Table 1
Baseline parameters for the numerical study.

Parameter	Value	Unit
a	5	mm
b	10	cm
k_x	10, 800	W/m/K
k_y	10, 800	W/m/K
$T_{c,in}$	10	°C
$T_{c,out}$	50	°C
$T_{h,in}$	90	°C
$T_{h,out}$	60	°C
$\bar{h}_h$	600	W/m^2/K
$\bar{h}_c$	400	W/m^2/K

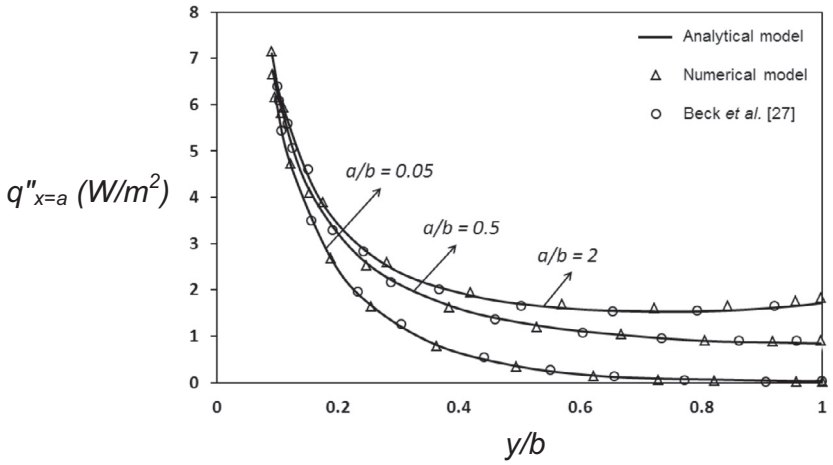

Fig. 3. Verification of the analytical model with the numerical and existing data, constant surface temperature, $k_x = k_y$.

of PHE. To conduct the parametric study, typical baseline properties, presented in Table 1, are considered. To obtain the temperature and heat flux distribution through the plate, the series solution from Eq. (4)is used. A code in C++ is developed to calculate the series solution for 50 terms. Using more terms does not affect the results up to four decimal digits. Different thermal conductivity combinations are considered for the orthotropic plate [14–16]. In Fig. 4, temperature distribution contours are presented for following three case studies:

- Case I: $k_x = k_y = 10$ W/m/K.
- Case II: $k_x = 800$, $k_y = 10$ W/m/K.
- Case III: $k_x = 10$, $k_y = 800$ W/m/K.

In addition, Fig. 5 shows the heat flux patterns for the above cases. From Fig. 4, one can conclude that by changing k_x from 10 to 800 W/m/K when k_y is kept constant (10 W/m/K), the temperature contour and its range throughout the plate is not changing significantly. This is a result of small thermal resistance of the considered thin plate even with low k_x values. However, by increasing k_y from 10 to 800 W/m/K, the temperature distribution throughout the plate changes significantly as expected. In fact, by increasing k_y, the in-plane heat transfer (the y-direction heat transfer) increases and results in a lower temperature difference between the top and bottom parts of the plate. In case III ($k_y = 800$ W/m/K), the temperature difference throughout the plate is less than 2 °C, while it is more than 20 °C for cases I and II ($k_y = 10$ W/m/K). It indicates that changing k_y would significantly affect the temperature distribution throughout the plate while the trend is completely reverse for k_x. As shown in Fig. 5, the effect of k_y (in-plane thermal conductivity) on the temperature range remarkably affects the heat transfer pattern through the plate. Fig. 5 also shows that by increasing k_x value from 10 to 800 for a constant $k_y = 10$ W/m/K, the heat flux patterns become nearly 1-D (x-direction) between hot and cold surfaces. This occurs as a result of a large thermal conductivity in the x-direction.

Similar results are observed for large values of k_y. From Fig. 5 one can observe that for large k_y values, as a result of a small in-plane thermal resistance (along the y-direction), the heat conduction becomes almost 1-D from the hot to the cold boundary. These

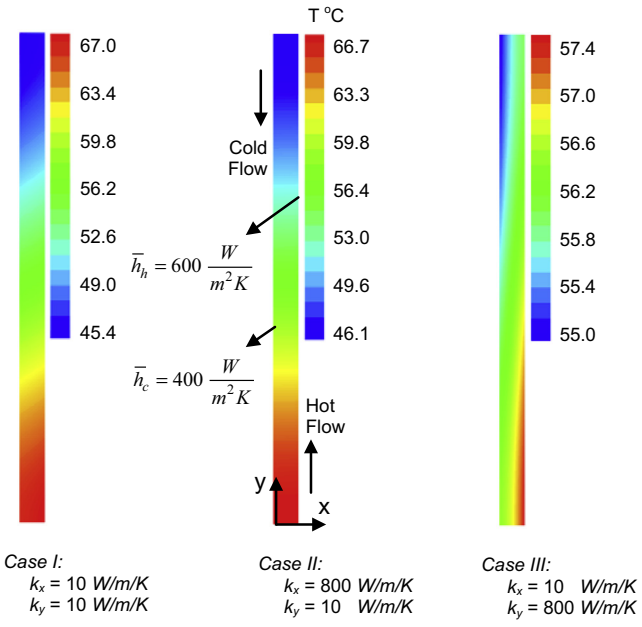

Fig. 4. Analytical solution for temperature distribution with different k_x, k_y ratios, Eq. (4), see Table 1 for other parameters.

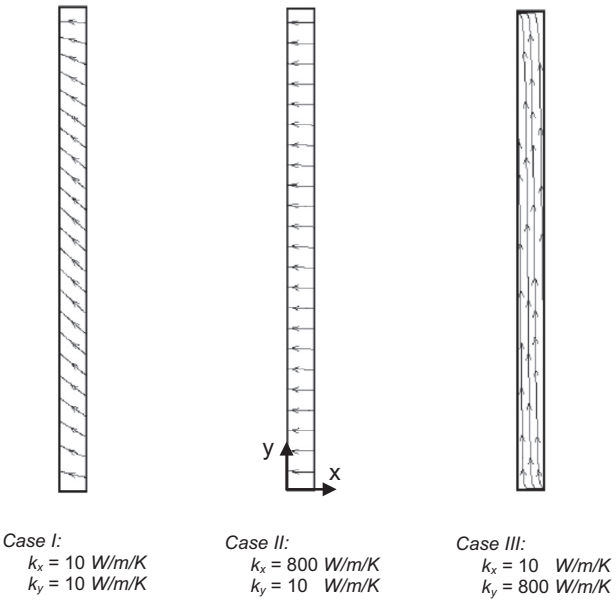

Fig. 5. Analytical solution for heat flux distribution with different k_x, k_y ratios, Eq. (9), see Table 1 for other parameters.

results show the importance of the orthotropicity in the temperature distribution and heat flux pattern in PHE.

It should be noted that the streams' bulk temperature variations ($T_m = T_c(y)$ for cold stream and $T_m = T_h(y)$ for hot stream) are considered to be the same for all the presented case studies. This assumption is completely different and more realistic than a fixed wall temperature (Dirichlet) or heat flux (Neumann) boundary conditions for a plate since controlling the fluid temperature is

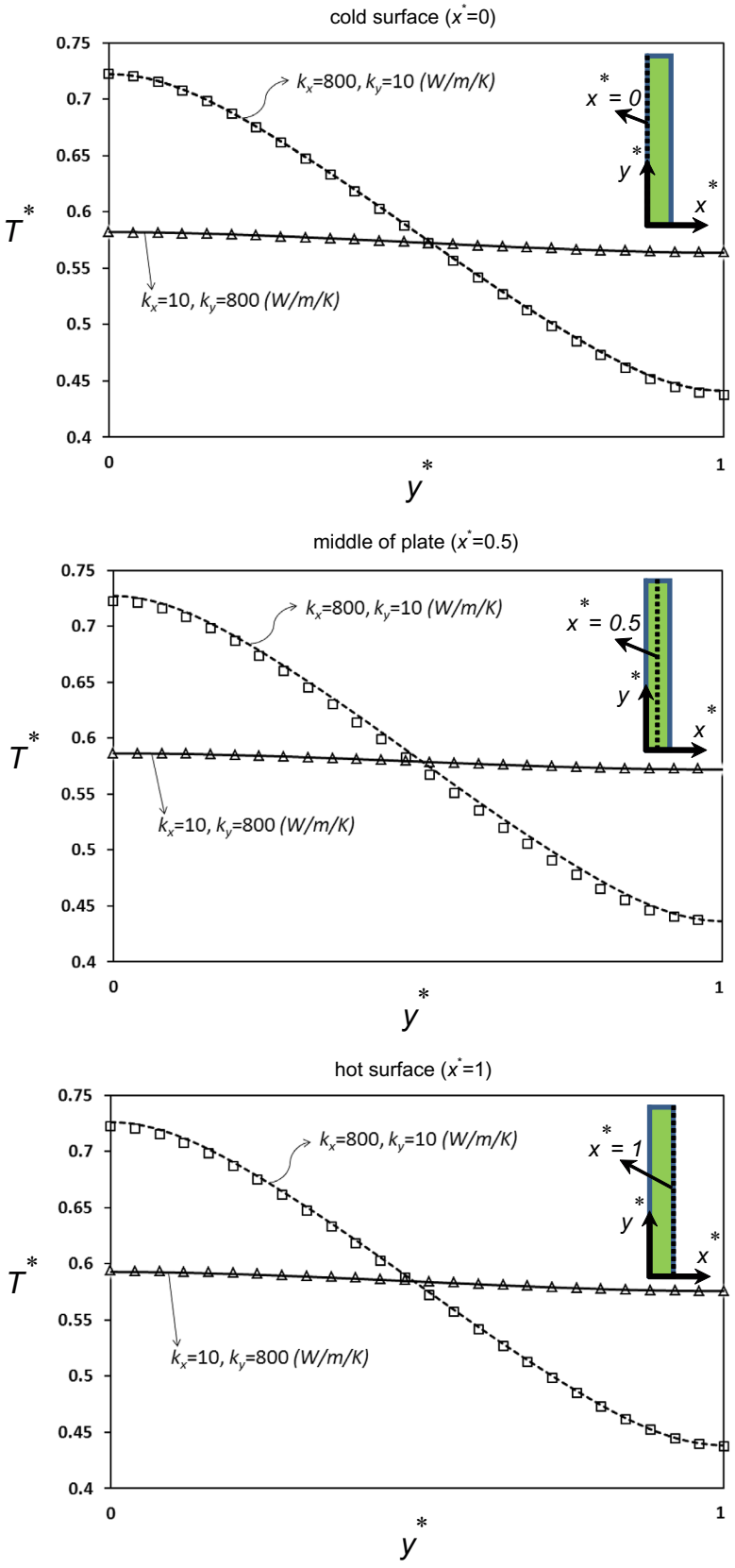

Fig. 6. Dimensionless longitudinal temperature profiles: analytical model (lines) and numerical results (symbols).

more feasible than wall temperature or heat flux in plate heat exchangers [1,4]. The local heat flux at any cross section (y = *constant*) is a function of fluid's thermal conductivity and the temperature gradient in x direction as presented in Eq. (13). Fixing the fluid's bulk temperature for different case studies does not mean that the temperature gradient is also fixed.

$$q''_x = -k\frac{\partial T}{\partial x}\bigg|_{x=0,a} = h(T_m - T(x,y)) \tag{13}$$

The right-hand side of Eq. (13) also indicates that the heat flux is a function of convective heat transfer coefficient h, bulk temperature T_m as well as the plate's wall temperature $T(x,y)$. Accordingly, a similar bulk temperature does not impose an identical heat flux for different case studies since the solid wall temperature does not remain the same. To apply the same fluid side's bulk temperature distribution ($T_c(y)$, $T_h(y)$) for all the case studies, the streams mass flow rate should be adjusted. In other words, for each case study it is assumed that by changing the streams' flow rate, the bulk temperature distributions are kept the same to focus only on the effects of orthotropicity on the conduction heat transfer domain.

For convenience and generality, dimensionless temperature profiles and heat flux distributions through the plate are defined as follows:

$$\begin{cases} T^* = \frac{T-T_{c,in}}{T_{h,in}-T_{c,in}} \\ x^* = \frac{x}{a} \\ y^* = \frac{y}{b} \\ q^* = \frac{q''}{h_h(T_{h,in}-T_{c,in})} \\ Q^* = \frac{Q}{h_h b(T_{h,in}-T_{c,in})} \end{cases} \tag{14}$$

Using the defined dimensionless parameters, Fig. 6 shows the temperature profiles on the cold surface (x = 0), the middle of the plate ($x = a/2$), and the hot surface ($x = a$) for cases II and III. The profiles show a good agreement between the analytical and numerical solutions. The maximum relative difference between the analytical results, Eqs. (4)–(9), and the obtained numerical data is less than 4%. As a result of thin plate thickness, the temperature profiles at different vertical planes (x-constants) have almost similar trends.

Analogous to the temperature distribution in Fig. 4, comparison between the results of cases II (k_x = 800, k_y = 10 W/m/K) and III (k_x = 10, k_y = 800 W/m/K) with switched thermal conductivity combinations implies that by increasing k_y, the temperature difference decreases throughout the plate. These profiles show that the dimensionless temperature for smaller k_y values varies in the range of 0.42–0.72, while its range for the large value of k_y is 0.56–0.60.

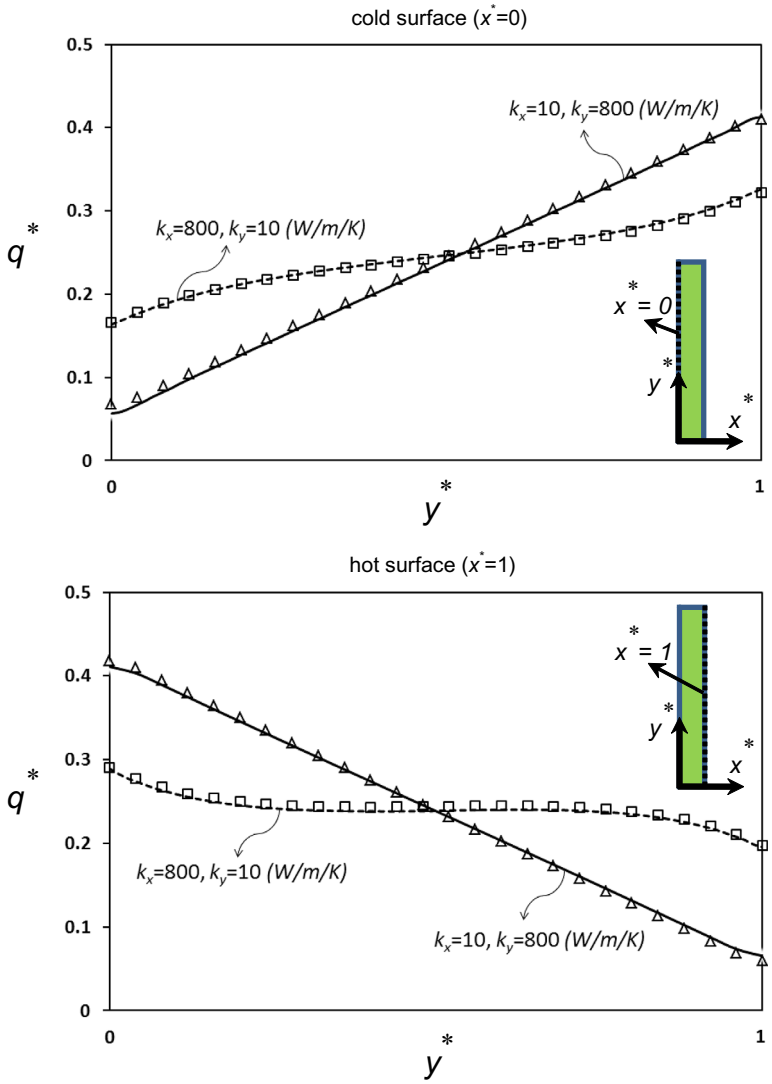

Fig. 7. Dimensionless surface heat flux profiles: analytical model (lines) and numerical results (symbols).

In Fig. 7, the heat flux distributions on the cold and hot surfaces of the plate are presented for the cases II and III. These results indicate a good agreement between the analytical and numerical solutions. As expected, the maximum heat flux at each surface of the plate occurs at the location with the maximum temperature difference between the fluid flow and the solid surface. The profiles show that for the cold surface (i.e. $x^* = 0$), the maximum heat flux occurs at $y^* = 1$ which is where the cold fluid flow meets the plate with the maximum temperature difference between solid and fluid. Moreover, for the hot surface (i.e. $x^* = 1$), this maximum temperature gradient and heat flux occurs at $y^* = 0$. Comparing the heat flux profiles for these two orthotropic thermal conductivity ratios indicates that, in spite of the same fluid side boundary conditions, the heat flux behavior will be completely different due to the effects of orthotropic thermal conductivities on the temperature distribution throughout the plate.

Cross sectional temperature profiles on different horizontal planes (y-constants) for the cases II ($k_x = 800$, $k_y = 10$ W/m/K) and III ($k_x = 10$, $k_y = 800$ W/m/K), are presented in Fig. 8. The profiles show that for the large value of $k_x = 800$ W/m/K temperature drop across the plate is relatively small. Indeed, the high rate of heat transfer across the plate – due to the small thermal resistance – keeps the temperature profiles nearly constant. However, the temperature values at $x^* = 0$ and $x^* = 1$ cannot be the same, since a small gradient is necessary for heat transfer across the plate.

Our results indicate that orthotropic thermal conductivity can significantly affect the total heat transfer rate in a slab between two fluid streams. The effectiveness of any heat exchanger is directly proportional to the total heat transfer rate between its fluid sides. For the same inlet fluid conditions, a higher total heat transfer rate between hot and cold flows results in a higher effectiveness of the heat exchanger [4].

To find out the effects of orthotropic thermal conductivity of the plate on the total heat transfer between the fluid sides, Fig. 9 is presented. The curves in Fig. 9 show the heat transfer behavior of the plate with various through-plane thermal conductivity for different convective heat transfer coefficients ($\bar{h}$) ranging from 5 W/m^2/K (~natural convection) to 5000 W/m^2/K (turbulent forced convection). The average convective heat transfer coefficient ($\bar{h}$) is defined in Eq. (15) and represents an average value of the fluid sides, surrounding the solid surfaces of the plate.

$$\frac{1}{\bar{h}} = \frac{1}{2}\left(\frac{1}{\bar{h}_h} + \frac{1}{\bar{h}_c}\right) \tag{15}$$

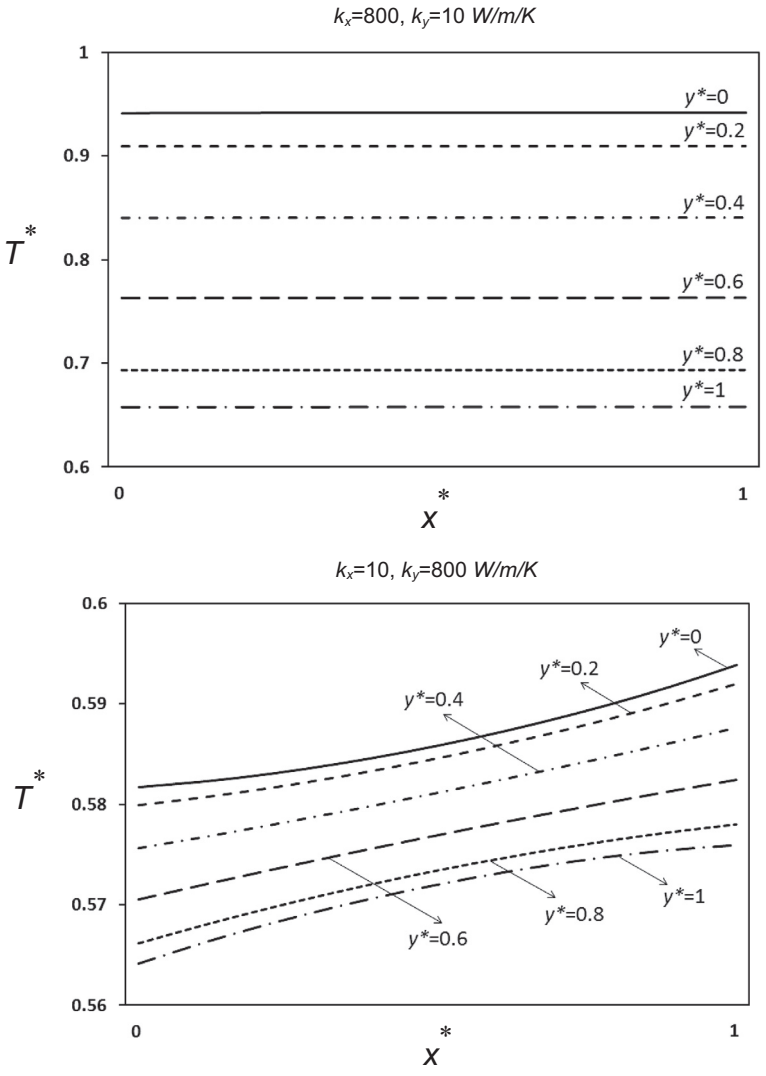

Fig. 8. Dimensionless cross sectional temperature profiles, analytical model.

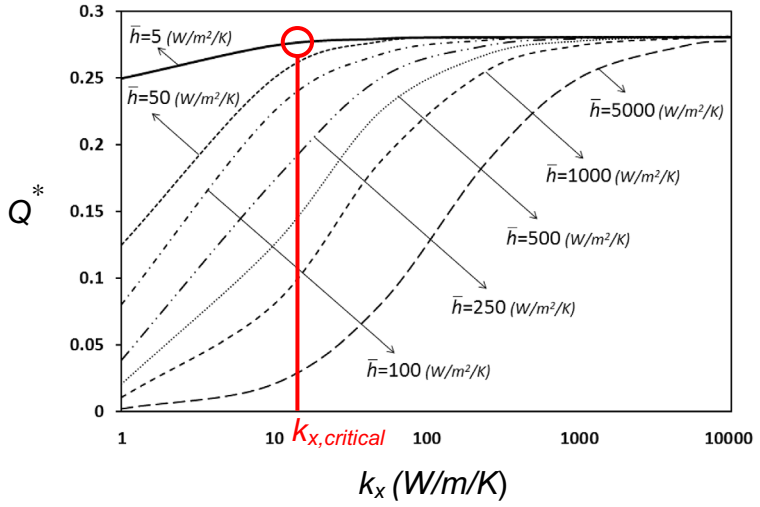

Fig. 9. Heat transfer across the orthotropic plate, analytical model: for each $\bar{h}$, there is a critical conductivity $k_{x,critical}$ beyond which increasing k_x does not considerably change the heat transfer rate between the fluid streams.

The vertical axis in Fig. 9 represents the dimensionless total heat transfer between the streams via the solid plate which is defined in Eq. (14). Based on Eqs. (14), (11), and (7), this dimensionless parameter is a function of fluid side properties as well as the plate's dimensions and through-plane thermal conductivity. Based on the obtained mathematical correlations, although the in-plane conductivity changes the general temperature contours, it does not affect the total heat transfer rate through the plate. Accordingly, for the specific plate defined in Table 1, by changing the plate's through-plane thermal conductivity while the fluid side thermal specifications are kept constant ($\bar{h}$ constant), the variations of total heat transfer rate are plotted in Fig. 9.

The curves in Fig. 9 show a higher rate of heat transfer enhancement at lower values of the conductivity. However, beyond some values of k_x, the heat transfer enhancement becomes negligible. It means that for each convective thermal resistance (constant-$\bar{h}$ curves), there is a "critical" or optimum through-plane conductivity, $k_{x,critical}$, beyond which increasing k_x does not change the heat transfer rate between fluid streams. This critical value exists since the convective heat transfer resistance controls the heat transfer. Indeed, by increasing k_x regardless of k_y value, the conductive thermal resistance of the plate reduces, and beyond a critical value, this resistance becomes negligible in comparison with the convective resistance. In other words, beyond the critical through-plane thermal conductivity, the convective thermal resistance controls the heat transfer between the hot and cold fluid streams and further increase in the through-plane conductivity does not change the performance of PHE.

Fig. 9 also indicates that by increasing the convective heat transfer coefficient ($\bar{h}$ value) – i.e. reducing the convective resistance – the value of the $k_{x,critical}$ will increase. Accordingly, the higher through-plane thermal conductivity k_x will be more beneficial for applications with higher convective heat transfer coefficients, e.g. boiling/condensation.

The critical value of k_x is correlated to the convective heat transfer coefficient in this study. Defining the critical k_x as the value beyond which the thermal resistance of the plate becomes less than 10% of the convective resistance in the system, Eq. (16) is derived:

$$\frac{a}{k_{x,critical}b} = 0.1\left(\frac{1}{\bar{h}_h b} + \frac{1}{\bar{h}_c b}\right) \tag{16}$$

After simplifications, Eq. (17) is obtained to calculate the $k_{x,critical}$ as a function of the plate thickness (a) and the characteristic convective heat transfer coefficient (h).

$$k_{x,critical} = \frac{10a}{\frac{1}{\bar{h}_h} + \frac{1}{\bar{h}_c}} = 5a\bar{h} \tag{17}$$

where $\bar{h}$, defined in Eq. (15), represents the average convective heat transfer coefficient. Eq. (17) shows that by increasing $\bar{h}$, the critical through-plane thermal conductivity ($k_{x,critical}$) increases linearly for any plate thickness. Consequently, using materials with higher through-plane thermal conductivity to manufacture the plates for two-phase PHE, e.g. evaporators and condensers, will provide higher effectiveness in comparison with single-phase heat exchangers. For instance, if a single-phase PHE with hot and cold water flows having an average convective heat transfer coefficient equal to 5000 W/m^2/K is built from plates with 2 mm thickness, the critical conductivity will be 50 W/m/K. It means that using a material with thermal conductivity higher than 50 W/m/K for the plates does not considerably change the effectiveness of the heat exchanger. However, for higher convective heat transfer coefficients such as; 50,000 W/m^2/K which appears in two-phase PHE, the critical through-plane conductivity will be 500 W/m/K. It means that for a two-phase heat exchanger, replacing the common aluminum plates, k = 100–200 W/m/K, with graphite-based plates, k_x = 500 W/m/K and higher, will considerably improve the effectiveness of the heat exchanger. In addition, the results show that for any PHE there is no need to increase k_x beyond the obtained critical value. Consequently, for each application there will be an optimum through-plane conductivity to achieve the highest heat exchanger effectiveness based on the fluid side operating conditions.

6. Conclusions

A new analytical model was developed for the heat conduction through orthotropic media, with a focus on emerging graphite-based plate heat exchangers (PHE) applications. Position-dependent heat flux boundary conditions were considered for orthotropic plates to develop a realistic model for the typical PHE and investigate the impact of orthotropicity of such plates. A method of separation of variables was applied to obtain the temperature and heat flux distributions through orthotropic plates. COMSOL Multiphysics was used to conduct an independent

numerical simulation for verifying the proposed analytical model. The results were also compared to the existing data from open literature and showed a great agreement with less than 5% discrepancy. The results of the study showed that different orthotropic in-plane and through-plane thermal conductivity combinations had significant effects on the heat flux and temperature distribution through orthotropic plates. A new "critical" through-plane conductivity was defined that demarcates the value beyond which the conductive thermal resistance becomes less than 10% of the convective resistance. This critical through-plane conductivity value was correlated to the average convective heat transfer coefficient of the fluid sides and the plate thickness. Using the proposed analytical model, a comprehensive parametric study was performed and the following was concluded:

- At smaller values of the through-plane thermal conductivity, by increasing this value the heat transfer rate through the slab will significantly increases. However, beyond the proposed critical value, increasing the through-plane conductivity has a negligible effect on the total heat transfer rate.
- Beyond the critical through-plane conductivity, the convective thermal resistance will control the total heat transfer rate between fluid streams.
- Using materials with high through-plane conductivity for applications with higher convective heat transfer coefficients, such as two-phase PHE: evaporators, condensers, will lead to greater effectiveness in comparison with single-phase PHE.
- For designing graphite-based PHE with highest effectiveness, the larger thermal conductivity should be in the through-plane direction, i.e. the direction of heat flow between the cold and hot fluid streams.

Conflict of interest

None declared.

References

[1] M.N. Ozisik, Heat Conduction, second ed., John Wiley & Sons, New York, 1993.
[2] H.S. Carslaw, J.C. Jaeger, Conduction of Heat in Solids, Oxford Press, 1959.
[3] V.S. Arpaci, Conduction Heat Transfer, Addison-Wesley Publishing Company, 1966.
[4] R.K. Shah, D.P. Sekulic, Fundamentals of Heat Exchanger Design, John Wiley & Sons, 2003.
[5] S. Kakac, H. Liu, Heat Exchangers: Selection, Rating, and Thermal Design, second ed., CRC Press, 2002.
[6] M. Mazen, A. Khader, Plate heat exchangers: recent advances, Renew. Sustain. Energy Rev. 16 (2012) 1883–1891.
[7] M. Vera, A. Liñán, Laminar counterflow parallel-plate heat exchangers: exact and approximate solutions, Int. J. Heat Mass Transfer 53 (2010) 4885–4898.
[8] J.A.W. Gut, J.M. Pinto, Modeling of plate heat exchangers with generalized configurations, Int. J. Heat Mass Transfer 46 (2003) 2571–2585.
[9] Q. Wang, X.H. Han, A. Sommers, Y. Park, C. T' Joen, a. Jacobi, A review on application of carbonaceous materials and carbon matrix composites for heat exchangers and heat sinks, Int. J. Refrig. 35 (2012) 7–26.
[10] Y. Gogotsi, Controlling graphene properties through chemistry, J. Phys. Chem. Lett. 2 (2011) 2509–2510.
[11] A. Heltzel, C. Mishra, R.S. Ruoff, A. Fleming, Analysis of an ultrathin graphite-based compact heat exchanger, Heat Transfer Eng. 33 (2012) 947–956.
[12] K.F. Kelly, W.E. Billups, Synthesis of soluble graphite and graphene, Acc. Chem. Res. 46 (2013) 4–13.
[13] P.V. Kamat, Graphene-Based nanoassemblies for energy conversion, J. Phys. Chem. Lett. 2 (2011) 242–251.
[14] J. Tersoff, Empirical interatomic potential for carbon with applications to amorphous carbon, Phys. Rev. Lett. 61 (1988) 2879–2882.
[15] <http://www.terrellaenergy.com/>.
[16] Z. Wei, Z. Ni, K. Bi, M. Chen, Y. Chen, In-plane lattice thermal conductivities of multilayer graphene films, Carbon N.Y. 49 (2011) 2653–2658.
[17] B. Mortazavi, S. Ahzi, Thermal conductivity and tensile response of defective graphene: a molecular dynamics study, Carbon N.Y. 63 (2013) 460–470.
[18] K.M.F. Shahil, A.A. Balandin, Thermal properties of graphene and multilayer graphene: applications in thermal interface materials, Solid State Commun. 152 (2012) 1331–1340.
[19] M. Zhao, Y. Li, New integral-mean temperature difference model for thermal design and simulation of parallel three-fluid heat exchanger, Int. J. Therm. Sci. 59 (2012) 203–213.
[20] J.A.W. Gut, R. Fernandes, J.M. Pinto, C.C. Tadini, Thermal model validation of plate heat exchangers with generalized configurations, Chem. Eng. Sci. 59 (2004) 4591–4600.
[21] B. Mathew, H. Hegab, Experimental investigation of thermal model of parallel flow microchannel heat exchangers subjected to external heat flux, Int. J. Heat Mass Transfer 55 (2012) 2193–2199.
[22] B. Prabhakara Rao, P. Krishna Kumar, S.K. Das, Effect of flow distribution to the channels on the thermal performance of a plate heat exchanger, Chem. Eng. Process. Process Intensification 41 (2002) 49–58.
[23] A. Durmuş, H. Benli, İ. Kurtbaş, H. Gül, Investigation of heat transfer and pressure drop in plate heat exchangers having different surface profiles, Int. J. Heat Mass Transfer 52 (2009) 1451–1457.
[24] Y.Y. Kim, K.S. Kim, G.H. Jeong, S. Jeong, An experimental study on the quantitative interpretation of local convective heat transfer for a plate fin and tube heat exchanger using the lumped capacitance method, Int. J. Heat Mass Transfer 49 (2006) 230–239.
[25] H.-T. Chen, J.-R. Lai, Study of heat-transfer characteristics on the fin of two-row plate finned-tube heat exchangers, Int. J. Heat Mass Transfer 55 (2012) 4088–4095.
[26] D. Dović, B. Palm, S. Švaić, Generalized correlations for predicting heat transfer and pressure drop in plate heat exchanger channels of arbitrary geometry, Int. J. Heat Mass Transfer 52 (2009) 4553–4563.
[27] M. Mehrabian, Math. Heat Transfer 23 (1998) 233–241.
[28] M. Mehrabian, R. Poulter, Appl. Math. Model. 24 (2000) 343–364.
[29] A. Grine, J.Y. Desmons, S. Harmand, Models for transient conduction in a flat plate subjected to a variable heat flux, Appl. Therm. Eng. 27 (2007) 492–500.
[30] J.V. Beck, N.T. Wright, A. Haji-Sheikh, K.D. Cole, D.E. Amos, Conduction in rectangular plates with boundary temperatures specified, Int. J. Heat Mass Transfer 51 (2008) 4676–4690.
[31] Y.V. Nemirovskii, A.P. Yankovskii, A method of asymptotic expansions of the solutions of the steady heat conduction problem for laminated non-uniform anisotropic plates, J. Appl. Math. Mech. 72 (2008) 92–101.
[32] M. Hsieh, C.C. Ma, Analytical investigations for heat conduction problems in anisotropic thin-layer media with embedded heat sources, Int. J. Heat Mass Transfer 45 (2002) 4117–4132.
[33] A. Bejan, Convection Heat Transfer, third ed., John Wiley & Sons, 2004.
[34] M. Lindstedt, R. Karvinen, Conjugate heat transfer in a plate – one surface at constant temperature and the other cooled by forced or natural convection, Int. J. Heat Mass Transfer 66 (2013) 489–495.